Research article

NMR IN BIOMEDICINE

Received: 25 August 2011, Revised: 16 March 2012, Accepted: 18 March 2012, Published online in Wiley Online Library: 27 April 2012

(wileyonlinelibrary.com) DOI: 10.1002/nbm.2806

# Intracerebral injection of human mesenchymal stem cells impacts cerebral microvasculature after experimental stroke: MRI study

**Anaïck Moisan[a,b,c]*, Nicolas Pannetier[a,b], Emmanuelle Grillon[a,b], Marie-Jeanne Richard[c,d,e], Florence de Fraipont[d,e], Chantal Rémy[a,b], Emmanuel L. Barbier[a,b] and Olivier Detante[a,b,f]**

**Stroke, the leading cause of disability, lacks treatment beyond thrombolysis. The acute injection of human mesenchymal stem cells (hMSCs) provides a benefit which could be mediated by an enhancement of angiogenesis. A clinical autologous graft requires an hMSC culture delay incompatible with an acute administration. This study evaluates the cerebral microvascular changes after a delayed injection of hMSCs. At day 8 after middle cerebral artery occlusion (MCAo), two groups of rats received an intracerebral injection in the damaged brain of either 10 μL of cell suspension medium (MCAo-PBS, $n = 4$) or $4 \times 10^5$ hMSCs (MCAo-hMSC, $n = 5$). Two control groups of healthy rats underwent the same injection procedures in the right hemisphere (control-PBS, $n = 6$; control-hMSC, $n = 5$). The effect of hMSCs on the microvasculature was assessed by MRI using three parameters: apparent diffusion coefficient (ADC), cerebral blood volume (CBV) and vessel size index (VSI). At day 9, eight additional rats were euthanised for a histological study of the microvascular parameters (CBV, VSI and vascular fraction). No ADC difference was observed between MCAo groups. One day after intracerebral injection, hMSCs abolished the CBV increase observed in the lesion (MCAo-hMSC: 1.7 ± 0.1% *versus* MCAo-PBS: 2.2 ± 0.2%) and delayed the VSI increase (vasodilation) secondary to cerebral ischaemia. Histological analysis at day 9 confirmed that hMSCs modified the microvascular parameters (CBV, VSI and vascular fraction) in the lesion. No ADC, CBV or VSI differences were observed between control groups. At the stroke post-acute phase, hMSC intracerebral injection rapidly and transiently modifies the cerebral microvasculature. This microvascular effect can be monitored *in vivo* by MRI. Copyright © 2012 John Wiley & Sons, Ltd.**

**Keywords:** stroke; mesenchymal stem cells; cell therapy; angiogenesis; microvasculature; MRI

## INTRODUCTION

Stroke is the leading cause of disability (1). Ischemic stroke (80% of cases) occurs when arterial blood flow is interrupted and leads to an enhancement of blood vessel growth in order to ensure the metabolic demand. Beyond the narrow time window open for thrombolysis, only rehabilitation is effective. To reduce post-stroke handicap, cell therapy has recently emerged as a 'regenerative treatment' (2,3). Human mesenchymal stem cells (hMSCs) are nonhaematopoietic stromal cells, poorly immunogenic (4), that can be expanded in culture and administered under autologous conditions. They differentiate into several cell types, including neurons (5). Moreover, after systemic infusion, hMSCs are capable of homing to injured tissues (6). Pilot clinical trials suggest a good tolerance and a benefit of the intravenous injection of autologous hMSCs in patients after stroke (7–9).

In rodent models, functional benefit of hMSCs has been reported in two studies after intravenous injection at 3 h after stroke (10,11), in four studies at 6 h (12–15) and in six studies at 1 day (11,12,16–19). Only one study reported a benefit and a reduced infarct size after intracerebral injection at the subacute stage (at 7 days) (20). The mechanisms by which hMSCs benefit after stroke are not well understood. Angiogenesis could be one of them. Indeed, the increase in cerebral blood flow (CBF)

* *Correspondence to: A. Moisan, Equipe 5: Neuroimagerie Fonctionnelle et Perfusion Cérébrale, Grenoble Institut des Neurosciences (GIN), Centre de Recherche Inserm U836-UJF-CEA-CHU, BP 170, 38042 Grenoble Cedex 9, France.*
*E-mail: anaick.moisan@gmail.com*

a *A. Moisan, N. Pannetier, E. Grillon, C. Rémy, E. L. Barbier, O. Detante*
*INSERM, U836, Grenoble, France*

b *A. Moisan, N. Pannetier, E. Grillon, C. Rémy, E. L. Barbier, O. Detante*
*Université Joseph Fourier, Grenoble Institut des Neurosciences (GIN), Grenoble, France*

c *A. Moisan, M.-J. Richard*
*Grenoble University Hospital, Cell Therapy Unit, Grenoble, France*

d *M.-J. Richard, F. Fraipont*
*Grenoble University Hospital, UM Biochimie des Cancers et Biothérapies, Grenoble, France*

e *M.-J. Richard, F. Fraipont*
*INSERM, U823, Université Joseph Fourier, Albert Bonniot Institute, La Tronche, France*

f *O. Detante*
*Grenoble University Hospital, Stroke Unit, Department of Neurology, Grenoble, France*

**Abbreviations used:** *ADC, apparent diffusion coefficient; CBF, cerebral blood flow; CBV, cerebral blood volume; hMSC, human mesenchymal stem cell; MCAo, middle cerebral artery occlusion; PBS, phosphate-buffered saline; ROI, region of interest; USPIO, ultrasmall superparamagnetic iron particles; VSI, vessel size index.*

NMR IN BIOMEDICINE

that occurs within 1–2 weeks after stroke has been reported to be essential for oxygenation and nutriment support (21,22). Moreover, the number of new blood vessels in the lesion seems to be correlated with a longer survival in humans (23). In animals, angiogenesis and CBF enhancement seem to be correlated with functional benefit (11,13,14). In rats, several studies have supported the idea that hMSCs administered within 1 day after stroke enhance angiogenesis and vascular maturation after cerebral ischaemia (12–14,17). These studies showed increased angiogenesis using *ex vivo* techniques and *in vivo* using perfusion MRI (13,14). MRI showed a CBF increase 7 days after cerebral ischaemia (hMSCs being injected 6 h after occlusion) (13); CBF was further enhanced when hMSCs were transfected with vascular endothelial growth factor and angiopoietine-1 genes (14).

However, in all of these studies, the delay between the lesion and the intravenous hMSC injection was too short to be compatible with a clinical autologous application which requires an *ex vivo* cell culture delay. The aim of this study was to prove the significant effect of hMSCs on the cerebral microvasculature after injection at the subacute stage of stroke (8 days). hMSCs were injected intracerebrally, first to avoid the first-pass trapping of cells, particularly in lungs (6), thus limiting the loss of cells, and, second, to ensure the presence of cells in brain parenchyma. To obtain a longitudinal follow-up, we chose MRI. Indeed, MRI has recently been used by Lin *et al.* (24) to describe the cerebral vasculature using the cerebral blood volume (CBV) and the perfused vessel diameter (vessel size index, VSI) after cerebral ischaemia in rats during 21 days. In this study, we monitored CBV and VSI during 21 days in a rat model of stroke treated by an intracerebral injection of hMSCs 8 days after the lesion.

## MATERIALS AND METHODS

Our protocol was approved by the local ethics committee. All animal procedures conformed strictly to French government guidelines and were performed under permit nos. 380806 (for OD) and A3851610008 (for experimental and animal care facilities) from the French Ministry of Agriculture. Anaesthesia was induced by the inhalation of 5% isoflurane (Abbott Scandinavia AB, Solna, Sweden) in 30% $O_2$ in air, and maintained throughout all surgical and imaging procedures with 2–2.5% isoflurane through a facial mask.

### Middle cerebral artery occlusion (MCAo) model

Transient focal brain ischaemia was induced by intraluminal occlusion of the right MCA (25). Briefly, the right carotid arterial tree was isolated. A cylinder of melted adhesive (length, 2 mm; diameter, 0.38 mm) attached to a nylon thread (diameter, 0.22 mm) was advanced from the lumen of the external carotid artery into the internal carotid artery up to 5 mm after the external skull base. After 90 min of occlusion, rats were re-anaesthetised and the thread was removed. The rectal temperature was monitored and maintained at $37.0 \pm 0.5$ °C.

MCAo rats were awakened and tested for spontaneous circling and forelimb flexion during the occlusion period, and exhibited neurological deficits as a consequence of the ongoing cerebral ischaemia. Control rats showed no sign of deficit.

### Intracerebral administration of hMSCs and experimental groups

hMSCs were used to be consistent with an ongoing clinical trial. The use of hMSCs in rats was made possible because of their poor immunogenicity (4).

hMSCs were isolated from bone marrow aspirate from healthy donors who gave consent. Culture procedures were conducted according to previously described methods (26,27) and hMSCs were harvested after two passages.

We employed a routinely used procedure for intracerebral injection with fixed external stereotaxic coordinates that allowed the implantation of tumor cells with reproducible locations. Two sites of injection were used in order to further optimise the distribution of hMSCs in the lesion. Rats were maintained in a stereotaxic frame. A hole was drilled in the skull above the right striatum (3 mm right from the bregma). A 10-μL Hamilton syringe was filled with 10 μL of phosphate-buffered saline (PBS)–glutamine alone or $4 \times 10^5$ hMSCs in 10 μL PBS–glutamine, and was slowly pulled down: 5 μL were injected (2 μL/min) at 6 mm depth below the bregma (striatum) and, after a 3-min delay, 5 μL were injected at 3 mm depth below the bregma (cortex). No immunosuppressants were used.

Twenty Sprague Dawley male rats (Janvier, Le Genest-St-Isle, France), weighing 250–300 g, were stratified on the MRI-measured lesion volume to obtain similar average lesion volumes between groups, and were randomly allocated into four groups: group 1, rats underwent MCAo at day 0 (D0) and, at D8, received a 10-μL PBS–glutamine intracerebral injection (MCAo-PBS, $n = 4$); group 2, rats underwent MCAo at D0 and, at D8, received an intracerebral injection of $4 \times 10^5$ hMSCs (MCAo-hMSC, $n = 5$); group 3, healthy rats received PBS–glutamine intracerebral injection (control-PBS, $n = 5$); group 4, healthy rats received hMSC intracerebral injection (control-hMSC, $n = 6$). In a separate experiment, eight additional rats were euthanised at D9 for immunohistological study (MCAo-PBS, $n = 4$; MCAo-hMSC, $n = 4$). The experimental design of the study is presented in Fig. 1a.

### *In vivo* MRI experiments

All groups were followed by MRI (7 T, Bruker Avance III (Wissenbourg, France), Preclinical MRI Facility of Grenoble) for 21 days (Fig. 1b).

A $T_2$-weighted sequence (TR/TE = 2500/60 ms; voxel size, $234 \times 234 \times 1000$ μm$^3$) was acquired at D1, D7, D9, D14 and D21 to measure the lesion volume. The apparent diffusion coefficient (ADC) was mapped (spin echo planar imaging; TR/TE = 3000/29 ms; $b = 900$ s/mm$^2$; voxel size, $234 \times 234 \times 1000$ μm$^3$) for the three principal directions.

CBV and VSI (perfused vessel diameter) were measured at D7, D9, D14 and D21. CBV and VSI values were obtained using a steady-state approach (i.e. before and after contrast agent injection) (28,29). Briefly, a multi-gradient echo spin echo sequence (TR/TE = 4000/40 ms; seven echoes from 2.3 to 15.6 ms; voxel size, $234 \times 234 \times 1000$ μm$^3$; seven slices) was acquired, before and 2 min after intravenous injection (tail vein) of an intravascular iron-based contrast agent [ultrasmall superparamagnetic iron particles (USPIO; Sinerem®, Guerbet, Roissy, France; Combidex®, AMAG Pharmaceuticals, Inc., Lexington, MA, USA; 200μmol iron/kg body weight).



  

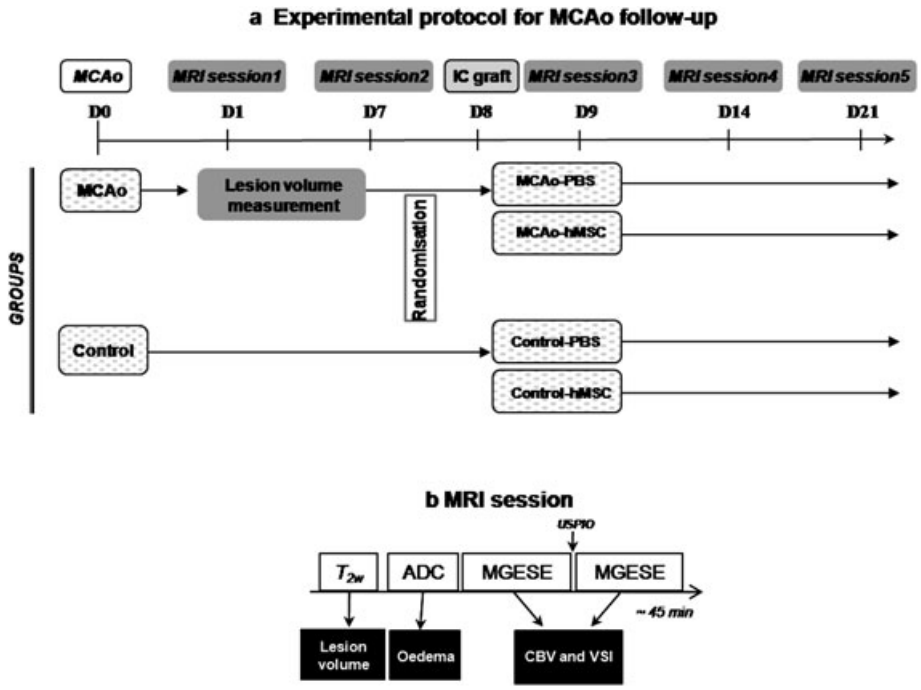


**Figure 1**. (a) Experimental protocol. At day zero (D0), nine rats underwent middle cerebral artery occlusion (MCAo) surgery with a 90-min occlusion and 11 rats did not undergo any surgery (control). At D8, animals were randomised and stratified into two MCAo groups with similar mean lesion volumes and two control groups. At D8, MCAo-PBS and control-PBS groups received an intracerebral (IC) injection of 10 μL of PBS–glutamine (cell suspension medium). At D8, MCAo-hMSC and control-hMSC groups received an IC injection of $4 \times 10^5$ human mesenchymal stem cells (hMSCs). All rats were imaged at each time point (D1, D7, D9, D14 and D21). Additional animals were killed at D9 for additional *ex vivo* experiments. (b) Diagram of the MRI session. ADC, apparent diffusion coefficient; CBV, cerebral blood volume; MGESE, multi-gradient echo spin echo; PBS, phosphate-buffered saline; $T_{2w}$, $T_2$-weighted; VSI, vessel size index.

### Immunohistology

Brains were removed, frozen and stored at −80 °C. Frozen brain tissue was cut with a cryostat (thickness, 10 μm). Eight coronal slices were generated per animal around the injection site. Slices were then incubated overnight at 4 °C with primary antibodies, washed with PBS and incubated (1 h) at room temperature with secondary antibodies.

Blood vessel quantification was performed using a primary antibody against endothelial cells (RecA, Serotec, Oxford, UK; 1 : 200) and an Alexa 488-linked donkey anti-mouse immunoglobulin G (Invitrogen, Eugene, OR, USA; 1 : 500). To identify human cells colocalised with blood vessels, double staining was employed. An antibody against human nuclei (HuNu, Abcys, Paris, France; 1 : 1000) and an antibody against von Willebrand factor (vWF, DakoCytomation, Glostrup, Denmark; 1 : 500) were used. An Alexa 488-linked donkey anti-mouse immunoglobulin G (Invitrogen; 1 : 500) and a rhodamine-conjugated donkey anti-rabbit immunoglobulin G (Jackson Laboratories, West Grove, PA, USA; 1 : 200) were used, respectively, for double-label-immunoreactivity. Images were obtained using epifluorescence microscopy (Nikon Eclipse E600, Tokyo, Japan) and a CCD camera (Olympus, Rungis, France).

### Data analysis

#### *MRI maps*

All maps were computed using a program developed in our laboratory within Matlab (MathWorks, Natick, MA, USA). For each rat at each MRI session, the whole ischaemic lesion was identified as the hyperintense area on contrast-optimised $T_2$-weighted images as proposed previously (30). The lesion was manually delineated consistently with neuroanatomy (e.g. excluding ventricles and/or small bleeding) and previous and next slices (12 slices in total). After delineation, the concordance of the delineated lesion with the ADC map was checked [lesion region of interest (ROI), Fig. 2b]. Lesion volumes were computed by adding the lesion areas of each slice. In control groups, ipsilateral ROIs were drawn in order to obtain a volume equal to the mean of all MCAo group lesion volumes for the corresponding MRI session. ADC values were measured in each ROI (seven slices per brain).

Changes in transverse relaxation rates caused by USPIO ($\Delta R_2^*$ and $\Delta R_2$) were obtained from gradient echo and spin echo signals acquired before and after USPIO injection. We used a fixed $\Delta\chi$ (0.191 ppm) and computed CBV and VSI maps as described by Tropres *et al.* (28). Mean CBV (%) and VSI (μm) values were then measured in ROIs.

To control the quality of CBV and VSI measurements over time, CBV and VSI were also estimated in the masseter muscle of each animal. To avoid any bias caused by the variability associated with the amount of injected USPIO, CBV and VSI values obtained from the brain were normalised by the CBV and VSI values measured in the masseter muscle, a reference used in perfusion studies (31,32). These ratios (further denoted as rCBV and rVSI) were calculated for each animal and each MRI session.

#### *Quantitative histology*

Quantitative analysis of blood vessels at D9 after MCAo was performed on RecA-immunostained sections (MCAo-PBS, $n = 4$;

NMR IN BIOMEDICINE

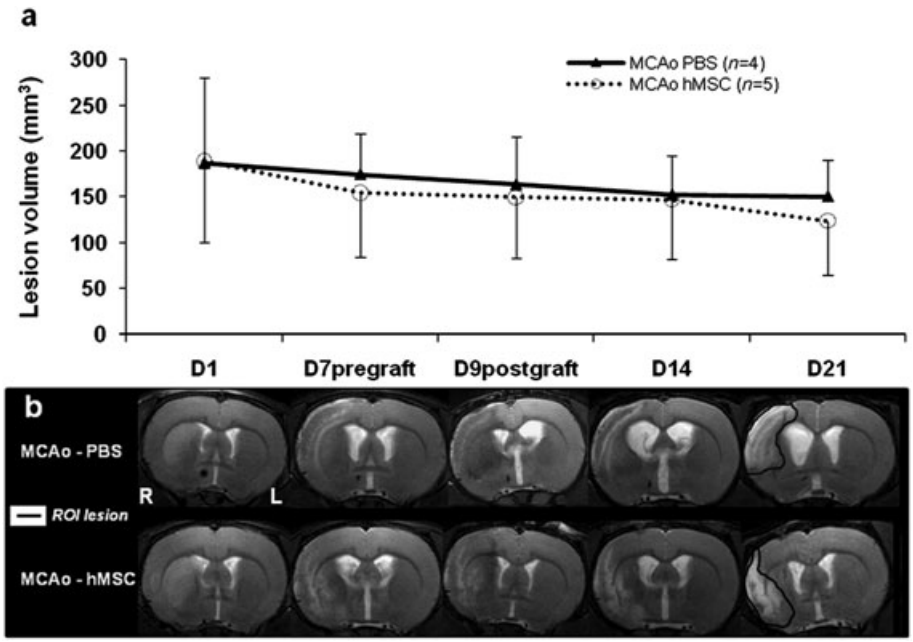


**Figure 2**. (a) Lesion volume over time in the MCAo-PBS ( ——▲—— ) and MCAo-hMSC ( ····○···· ) groups (mean ± standard error of the mean). (b) $T_2$-weighted maps from representative rats in the MCAo-PBS and MCAo-hMSC groups from D1 to D21. Example of lesion region of interest (ROI) delineated on $T_2$-weighted maps. hMSC, human mesenchymal stem cell; L, left hemisphere; MCAo, middle cerebral artery occlusion; PBS, phosphate-buffered saline; R, right hemisphere.

MCAo-hMSC, $n = 4$). Owing to considerable necrosis in the lesion, only striatal ROIs were acceptable for immunohistological analysis. Sections (one ROI/787.1 × 588.2 $\mu m^2$; eight slices/animal; Fig. 6a) were digitised using a CCD camera (Olympus). RecA images were binarised (threshold manually defined) and vascular parameters [vascular fraction (%), mean vessel radius ($r$) and mean vessel length ($h$)] were obtained using ImageJ software (Rasband, WS; ImageJ, National Institutes of Health, Bethesda, MD, USA). To allow comparison between MRI data and histological data, $VSI_{histo}$ (μm) and $CBV_{histo}$ (%) data were computed as described by Tropres *et al.* (33).

### Statistical analysis

Results are expressed as the mean ± standard error of the mean or mean ± standard deviation. Between-group comparison was performed using unpaired $t$-test after checking the variance homogeneity (Levene's test). Paired $t$-test was used for within-group comparison. In case of inhomogeneity of variance, a Mann–Whitney test was employed and its use is mentioned in the Results section. $p < 0.05$ was considered to be significant.

## RESULTS

No difference in weight was observed during the 21-days follow-up between hMSC-treated groups (MCAo-hMSC and control-hMSC) and PBS–glutamine groups (MCAo-PBS and control-PBS) (not shown). No adverse effect was observed in the daily behaviour of hMSC-treated animals.

### Lesion volume and oedema follow-up

MCAo groups (MCAo-PBS, MCAo-hMSC) exhibited a similar initial lesion volume (D1, 187 ± 195 $mm^3$ *versus* 189 ± 199 $mm^3$) and a similar evolution of the lesion volume during 3 weeks (Fig. 2). The lesion locations were similarly shared between the MCAo-PBS and MCAo-hMSC groups (MCAo-PBS, three cortico-striatal lesions and one striatal lesion; MCAo-hMSC, three cortico-striatal lesions and two striatal lesions). We did not observe any pure cortical lesion. As a result of the spatial resolution used in MRI, the needle path was almost never detectable.

We noted no difference in ADC between control-PBS and control-hMSC groups (Fig. 3). Ipsilateral ADC was lower at D1 for MCAo-PBS and MCAo-hMSC groups than for control groups [582 ± 191 $\mu m^2/s$ (Mann–Whitney) and 582 ± 38 $\mu m^2/s$ *versus* 835 ± 58 $\mu m^2/s$]. Ipsilateral ADC was higher at D14 and D21 for the MCAo-PBS group than for the control-PBS group (D14: 1059 ± 223 $\mu m^2/s$ *versus* 724 ± 63 $\mu m^2/s$, $p = 0.014$; D21: 1182 ± 221 $\mu m^2/s$ *versus* 806 ± 68 $\mu m^2/s$, $p = 0.008$). This confirms the presence of cytotoxic oedema at the acute stage of stroke, which gradually switches through vasogenic oedema at the later stage of stroke.

No ADC difference was observed between MCAo-PBS and MCAo-hMSC groups at D9, D14 and D21 (D9: 824 ± 233 $\mu m^2/s$ *versus* 763 ± 130 $\mu m^2/s$; D14: 1059 ± 223 $\mu m^2/s$ *versus* 1188 ± 522 $\mu m^2/s$; D21: 1182 ± 221 $\mu m^2/s$ *versus* 1336 ± 593 $\mu m^2/s$) (Fig. 3).

### Evolution of MRI cerebral vascular parameters

*CBV*

We noted no rCBV difference between control-PBS and control-hMSC groups (mean rCBV, 1.0 ± 0.1). At D7, no rCBV difference was observed between MCAo-PBS and MCAo-hMSC groups, demonstrating the homogeneity of the groups before treatment. In the MCAo-PBS group, rCBV in the lesion was higher than in control groups at D9, D14 and D21, with a peak at D9, and decreased between D14 and D21 (D7 *versus* D9: 1.3 ± 0.3 *versus* 2.2 ± 0.2, $p = 0.018$; D14 *versus* D21: 2.1 ± 0.3 *versus* 1.5 ± 0.3, $p = 0.008$). In the MCAo-hMSC group, rCBV in the lesion was also



  

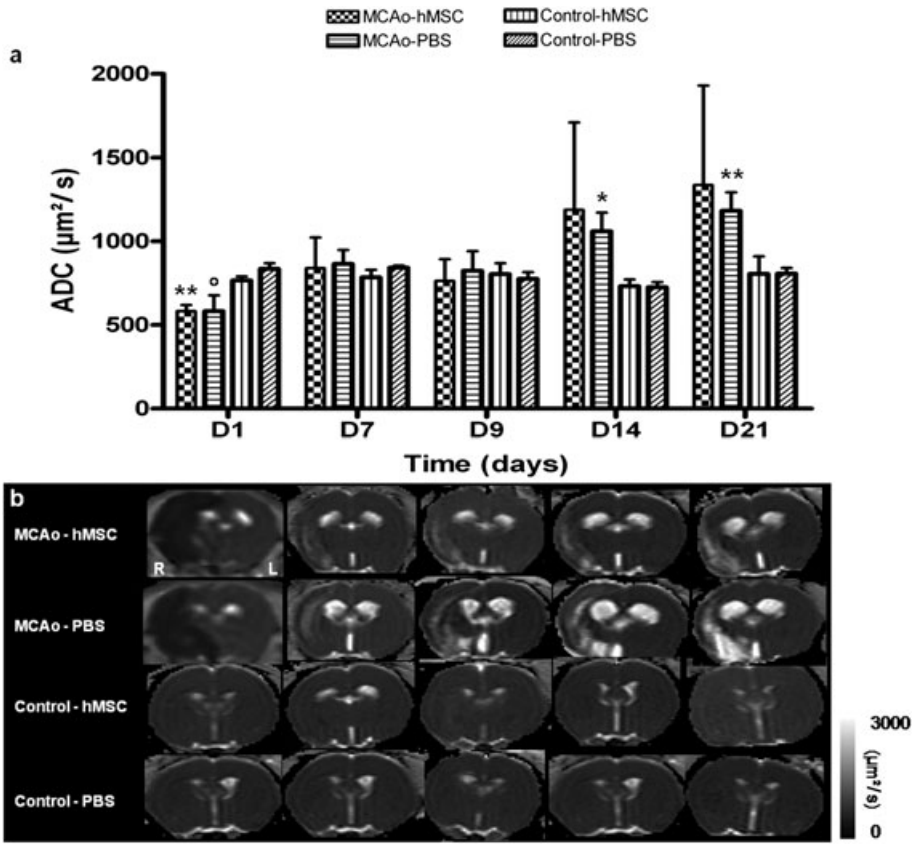


**Figure 3**. Apparent diffusion coefficient (ADC) over time after transient cerebral ischaemia and human mesenchymal stem cell (hMSC) intracerebral injection. (a) Quantitative analysis of ADC over time in the MCAo-hMSC, MCAo-PBS, control-hMSC and control-PBS groups in the ispilateral hemisphere (mean ± standard deviation). Differences between middle cerebral artery occlusion (MCAo) and control animals were significant at $*p < 0.05$ (*t*-test), $^{\circ}p < 0.05$ (Mann–Whitney) and $**p < 0.01$ (*t*-test) levels. (b) ADC maps from representative rats in the MCAo-hMSC, MCAo-PBS, control-hMSC and control-PBS groups from D1 to D21. L, left hemisphere; PBS, phosphate-buffered saline; R, right hemisphere.

higher than in control groups at D9, D14 and D21 without any peak at D9 and without a decrease between D14 and D21 (D7 *versus* D9: 1.4 ± 0.2 *versus* 1.7 ± 0.1, $p = 0.146$; D14 *versus* D21: 1.7 ± 0.2 *versus* 1.6 ± 0.1, $p = 0.390$). At D9, rCBV was higher in the MCAo-PBS group than in the MCAo-hMSC group (2.2 ± 0.2% *versus* 1.7 ± 0.1%, $p = 0.002$). At other time points, rCBV in the lesion was similar between the MCAo-PBS and MCAo-hMSC groups (Fig. 4).

*VSI*

We noted no difference in rVSI between control-PBS and control-hMSC groups (mean rVSI, 1.5 ± 0.2). At D7, no rVSI difference was observed between MCAo-PBS and MCAo-hMSC groups, demonstrating the homogeneity of the groups before treatment. At all time points, in the MCAo-PBS group, rVSI in the lesion was higher than in control groups with an increase at D9 (D7 *versus* D9: 2.9 ± 0.6 *versus* 4.0 ± 0.3, $p = 0.045$), which was still visible at D14 and D21 [MCAo-PBS *versus* control at D7 (Mann–Whitney): 2.9 ± 0.6 *versus* 1.5 ± 0.3, $p = 0.016$; D9: 4.0 ± 0.3 *versus* 1.6 ± 0.2, $p < 0.001$; D14 (Mann–Whitney): 3.8 ± 0.8 *versus* 1.5 ± 0.1, $p = 0.01$; D21 (Mann–Whitney): 3.2 ± 1.0 *versus* 1.5 ± 0.2, $p = 0.039$). At all time points, rVSI in the lesion was higher in the MCAo-hMSC group than in control groups, with an increase between D9 and D14 which remained stable afterwards (D9 *versus* D14: 2.9 ± 0.5 *versus* 3.9 ± 0.7, $p = 0.007$). At D9, rVSI in the lesion was higher in the MCAo-PBS group than in the MCAo-hMSC group (4.0 ± 0.3 *versus* 2.9 ± 0.5, $p = 0.003$). At other time points, rVSI was similar between these two groups (Fig. 5).

### Histological vascular parameters

At D9, $CBV_{histo}$, $VSI_{histo}$ and the total vascular fraction in the lesion were higher in the MCAo-PBS group than in the MCAo-hMSC group ($CBV_{histo}$: 8.1 ± 2.3% *versus* 5.6 ± 1.8%, $p < 0.001$; $VSI_{histo}$: 4.2 ± 0.6 µm *versus* 3.9 ± 0.5 µm, $p = 0.001$; total vascular fraction: 4.4 ± 0.9% *versus* 3.3 ± 0.8%, $p < 0.001$) (Fig. 6b–d). The $CBV_{histo}$ and $CBV_{MRI}$ results were closely similar in MCAo-PBS and MCAo-hMSC groups ($CBV_{histo}$ *versus* $CBV_{MRI}$: 8.1 ± 2.3% *versus* 6.3 ± 0.7%; 5.6 ± 1.8% *versus* 4.7 ± 0.1%). $VSI_{histo}$ was four times smaller than $VSI_{MRI}$ in the MCAo-PBS and MCAo-hMSC groups ($VSI_{histo}$ *versus* $VSI_{MRI}$ in the MCAo-PBS group: 4.4 ± 0.9 µm *versus* 16.3 ± 1.0µm; in the MCAo-hMSC group: 3.9 ± 0.5 µm *versus* 11.5 ± 1.4 µm).

The presence of a few human cells in the injected hemisphere was confirmed in the MCAo-hMSC group (Fig. 6f). No human cells were observed in groups that received an intracerebral administration of PBS (MCAo-PBS and control-PBS) (Fig. 6f). Human cells were preferentially found along ventricles and appeared around blood vessels (Fig. 7). In the lesion of hMSC-treated groups, a few human nuclei colocalised with endothelial cells.

NMR IN BIOMEDICINE

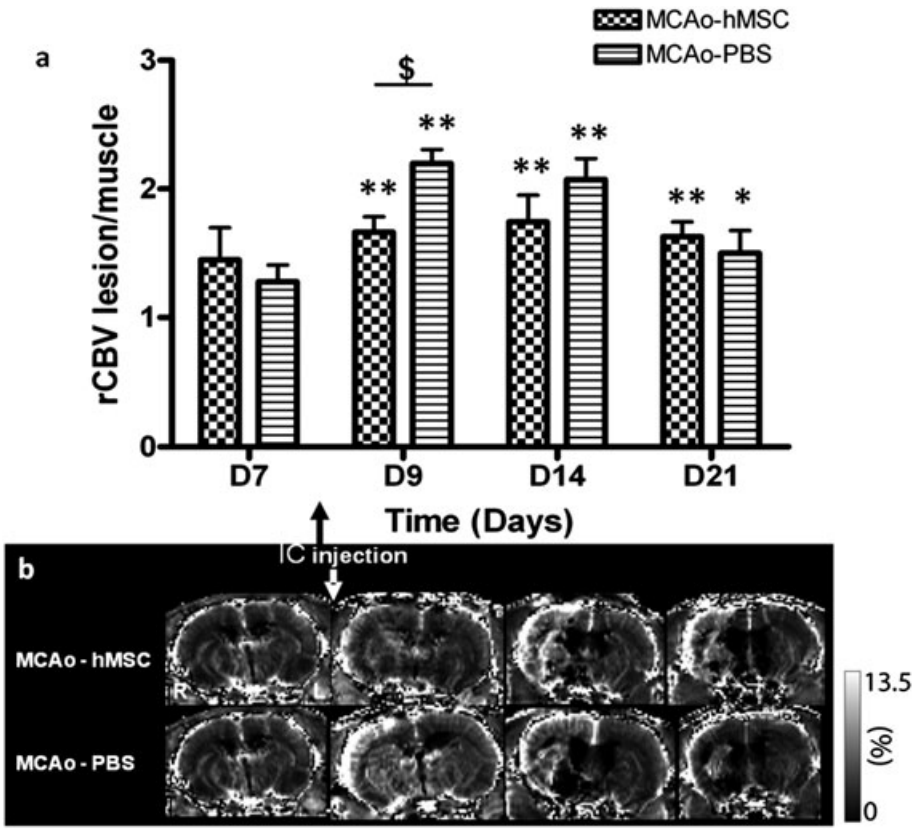


**Figure 4**. Effect of phosphate-buffered saline (PBS) and human mesenchymal stem cell (hMSC) intracerebral (IC) injection on the cerebral blood volume ratio (rCBV) after focal cerebral ischaemia. (a) Quantitative analysis over time of rCBV in MCAo-hMSC and MCAo-PBS groups (mean standard deviation). Differences between middle cerebral artery occlusion (MCAo) and control animals were significant at the $*p < 0.05$ (*t*-test) and $**p < 0.01$ (*t*-test) levels. Differences between MCAo-hMSC and MCAo-PBS were significant at the $\$p < 0.01$ (*t*-test) level. (b) CBV maps (%) from representative rats after hMSC or PBS–glutamine intracerebral injection from D7 to D21. L, left hemisphere; R, right hemisphere.

## DISCUSSION

After stroke, the microvascular characteristics of the lesion evolve. Our study shows that a delayed injection of hMSCs impacts this evolution of the microvasculature. To characterise this effect, we used *in vivo* MRI and *ex vivo* histology. Both approaches yield consistent results, despite a difference in absolute values between MRI and histology. This difference may be ascribed to numerous factors which have been discussed extensively in previous studies (28,29,31). MRI values obtained in control brains without lesions are comparable with those obtained previously in rat brain (31,34,35).

In the lesion of the MCAo-PBS group, rCBV was larger than in control animals with a peak at D9, and then decreased. rVSI was higher than in control animals at D7 and peaked at D9. Lin *et al*. (24,36) reported a similar trend using a three-vessel occlusion model (cortical lesions) but with earlier peaks (D3 and D7) in CBV and VSI. To evaluate the impact of the intracerebral injection procedure, we performed a sham experiment in four MCAo animals without any intracerebral injection. The evolution of rCBV and rVSI was similar to that observed after intracerebral injection of PBS (data not shown). This result indicates that the changes in microvascular parameters observed in the MCAo-PBS group cannot be ascribed to the intracerebral injection procedure, but are a normal evolution after transient cerebral ischaemia.

Our study demonstrates that the delayed intracerebral injection of hMSCs impacts the microvascular evolution after transient ischaemia. It would have been of interest to evaluate the functional benefit of hMSCs delivered intracerebrally. However, the objective of our study was to determine the effect of hMSCs on the evolution of the cerebral microvasculature after MCAo, based on the previously reported benefit of hMSCs delivered intracerebrally (20). When intravenously administered, hMSCs have been found to improve behavioural performance whatever the timing of cell injection after stroke. Chen *et al*. (5) reported a similar functional benefit (35 days after MCAo) of MSCs injected intravenously at 1 and 7 days after MCAo. According to Komatsu *et al*. (37), the intravenous administration of MSCs at 7 days, 14 days or 1 month after cerebral infarction results in an improvement in behavioural performance after 3 months, with no difference between the three timings of injection.

If the timing of injection does not influence the benefit of MSCs, the mechanisms involved might differ between early and delayed injection of cells, in line with the fact that hMSCs are well known to be regulated by their microenvironment (38).

When hMSCs are injected at the acute phase of stroke (6 h or 1 day), several studies have reported an improvement in CBF or an enhancement of angiogenesis. These studies used either perfusion MRI for 7 days (13,14) or *in vitro* techniques for 14 days



  

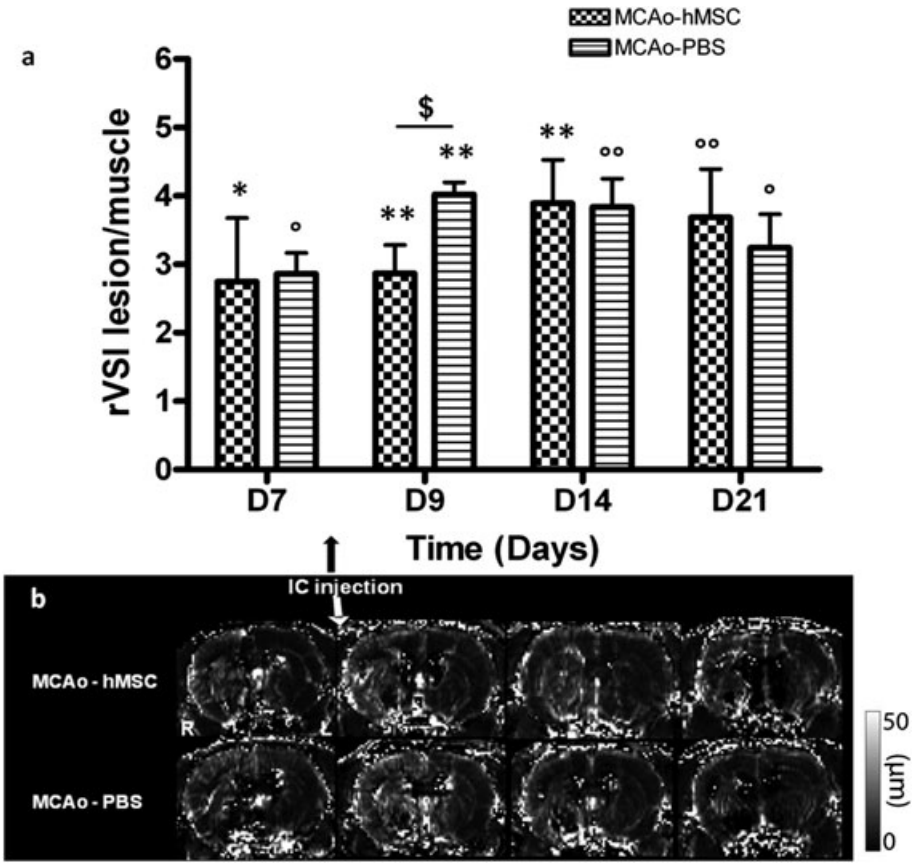


**Figure 5**. Effect of phosphate-buffered saline (PBS) and human mesenchymal stem cell (hMSC) intracerebral (IC) injection on the vessel size index ratio (rVSI) after focal cerebral ischaemia. (a) Quantitative analysis over time of rVSI in MCAo-hMSC and MCAo-PBS groups (mean ± standard deviation). Differences between middle cerebral artery occlusion (MCAo) and control animals were significant at the $^{*}p < 0.05$ (*t*-test), $^{\circ}p < 0.05$ (Mann–Whitney), $^{**}p < 0.01$ (*t*-test) and $^{\circ\circ}p < 0.01$ (Mann–Whitney) levels. Differences between MCAo-hMSC and MCAo-PBS were significant at the $\$p < 0.01$ (*t*-test) level. (b) VSI maps from representative rats after hMSC or PBS–glutamine intracerebral injection from D7 to D21. L, left hemisphere; R, right hemisphere.

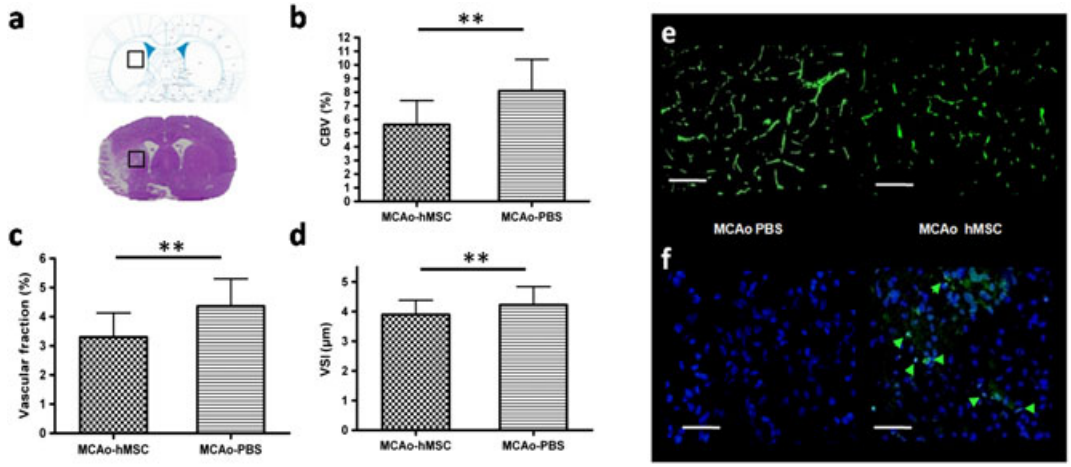


**Figure 6**. Histological vascular parameters at day 9 (D9). (a) Region of interest for vascular parameter measurement. Quantitative analysis of: (b) $CBV_{histo}$ (%); (c) vascular fraction (%); (d) $VSI_{histo}$ (µm) in the MCAo-hMSC ( ▩ ) and MCAo-PBS ( ▭ ) groups. $^{**}p < 0.001$ (*t*-test). (e) Photographs of RecA labelling (20×) in the MCAo-PBS and MCAo-hMSC groups. Scale bar, 100 µm. (f) Human cell labelling (HuNu). Human cells were present in the lesion of the MCAo-hMSC group, but not in that of the MCAo-PBS group (green arrows, human cells). Scale bar, 50 µm. CBV, cerebral blood volume; hMSC, human mesenchymal stem cell; MCAo, middle cerebral artery occlusion; PBS, phosphate-buffered saline; VSI, vessel size index.

(11–14,17). No study has reported any vascular effect of hMSCs injected at the subacute phase post-stroke. Our data suggest a novel dimension for hMSC injection at the subacute stage of stroke (8 days). One day after their intracerebral graft, hMSCs decreased rCBV at D9, delayed vasodilation from D9 to D14, and sustained the rCBV level after the graft (D9, D14 and D21).

This could be ascribed to a stabilisation effect from hMSCs on pre-existing vessels (39). Moreover, we showed that human cells

NMR IN BIOMEDICINE

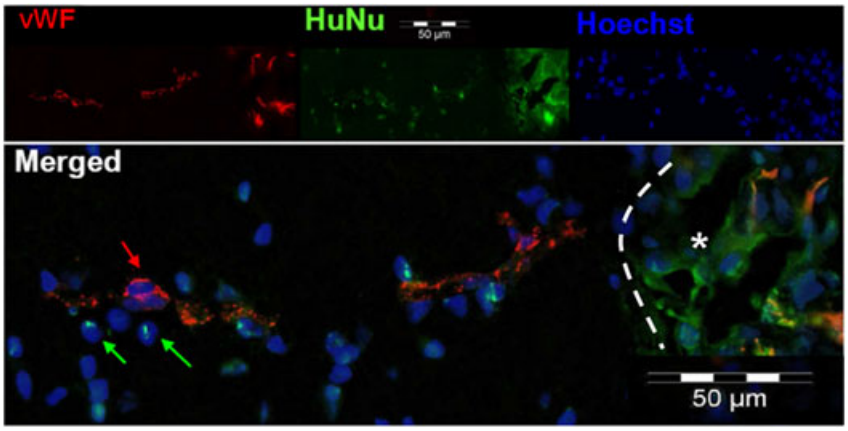


**Figure 7**. Double-labelled microphotographs for vWF/HuNu. Human cells were preferentially found along the ventricles (*, ventricular area) and appeared around the blood vessels (red arrows, blood vessels; green arrows, human cells). Scale bar, 50 µm.

preferentially pool around blood vessels, underlining the hypothesis that hMSCs can differentiate into 'supporting cells' which, via a paracrine mechanism (40), can stabilise pre-existing and newly formed vessels and respond to vasoactive stimuli (41). Human cells were also found in the periventricular zone, the favourite place linking angiogenesis and neurogenesis (42,43).

Another hypothesis is that lower rCBV and rVSI could be associated with a reduced number of inflammatory cells rolling through the endothelium and coming into the lesion, in line with the immunomodulatory properties of hMSCs (4,44). Moreover, it is well known that vasodilation after cerebral ischaemia can worsen the lesion as a result of increased inflammation (21,45), highly vascular regions being associated with an increased number of macrophages (46,47).

Our immunohistochemical data suggest a poor capacity of hMSCs to differentiate into endothelial cells, as reported previously (17,18). Therefore, this mechanism cannot contribute significantly to the effect of hMSCs on the cerebral microvasculature.

This study showed a significant effect of hMSCs on the cerebral microvasculature after stroke. Further studies are required to optimise cell delivery (injection route, effect of spatial and/or temporal fractionation). Mechanistic investigations (serial biological investigations) are needed in order to understand the observed microvascular evolution and the mechanisms involved in the effects of hMSCs on the cerebral microvasculature after stroke.

## CONCLUSIONS

We have demonstrated that MRI is suited to the study of the cerebral microvasculature *in vivo* and to the assessment of the effect of cell therapy on the microvasculature in stroke models. One day after intracerebral injection, hMSCs impacted the cerebral microvasculature and abolished the rCBV increase that occurred between 9 and 14 days after ischaemia. According to VSI data, hMSCs also delayed the vasodilation secondary to ischaemia.

## Acknowledgements

We thank the Preclinical MRI Facility of Grenoble, the Cell Therapy Unit and the UM Biochimie des Cancers et Biothérapies of Grenoble University Hospital for their friendly technical support. We are grateful to Guerbet (Roissy, France) for providing Sinerem®.

## REFERENCES

1. Lloyd-Jones D, Adams R, Carnethon M, De Simone G, Ferguson TB, Flegal K, Ford E, Furie K, Go A, Greenlund K, Haase N, Hailpern S, Ho M, Howard V, Kissela B, Kittner S, Lackland D, Lisabeth L, Marelli A, McDermott M, Meigs J, Mozaffarian D, Nichol G, O'Donnell C, Roger V, Rosamond W, Sacco R, Sorlie P, Stafford R, Steinberger J, Thom T, Wasserthiel-Smoller S, Wong N, Wylie-Rosett J, Hong Y. Heart disease and stroke statistics – 2009 update: a report from the American Heart Association Statistics Committee and Stroke Statistics Subcommittee. Circulation 2009; 119: 480–486.
2. Burns TC, Steinberg GK. Stem cells and stroke: opportunities, challenges and strategies. Expert Opin. Biol. Ther. 2011; 11: 447–461.
3. Lindvall O, Kokaia Z. Recovery and rehabilitation in stroke: stem cells. Stroke 2004; 35: 2691–2694.
4. Chamberlain G, Fox J, Ashton B, Middleton J. Concise review: mesenchymal stem cells: their phenotype, differentiation capacity, immunological features, and potential for homing. Stem Cells 2007; 25: 2739–2749.
5. Chen J, Li Y, Wang L, Zhang Z, Lu D, Lu M, Chopp M. Therapeutic benefit of intravenous administration of bone marrow stromal cells after cerebral ischemia in rats. Stroke 2001; 32: 1005–1011.
6. Detante O, Moisan A, Dimastromatteo J, Richard MJ, Riou L, Grillon E, Barbier E, Desruet MD, De Fraipont F, Segebarth C, Jaillard A, Hommel M, Ghezzi C, Remy C. Intravenous administration of Tc-99m-HMPAO-labeled human mesenchymal stem cells after stroke: in vivo imaging and biodistribution. Cell Transplant. 2009; 18: 1369–1379.
7. Bang OY, Lee JS, Lee PH, Lee G. Autologous mesenchymal stem cell transplantation in stroke patients. Ann. Neurol. 2005; 57: 874–882.
8. Lee JS, Hong JM, Moon GJ, Lee PH, Ahn YH, Bang OY. A long-term follow-up study of intravenous autologous mesenchymal stem cell transplantation in patients with ischemic stroke. Stem Cells 2010; 28: 1099–1106.
9. Honmou O, Houkin K, Matsunaga T, Niitsu Y, Ishiai S, Onodera R, Waxman SG, Kocsis JD Intravenous administration of auto serum-expanded autologous mesenchymal stem cells in stroke. Brain 2011; 134: 1790–1807.
10. Horita Y, Honmou O, Harada K, Houkin K, Hamada H, Kocsis JD. Intravenous administration of glial cell line-derived neurotrophic factor gene-modified human mesenchymal stem cells protects against injury in a cerebral ischemia model in the adult rat. J. Neurosci. Res. 2006; 84: 1495–1504.
11. Liu H, Honmou O, Harada K, Nakamura K, Houkin K, Hamada H, Kocsis JD. Neuroprotection by PlGF gene-modified human mesenchymal stem cells after cerebral ischaemia. Brain 2006; 129: 2734–2745.
12. Omori Y, Honmou O, Harada K, Suzuki J, Houkin K, Kocsis JD. Optimization of a therapeutic protocol for intravenous injection of human mesenchymal stem cells after cerebral ischemia in adult rats. Brain Res. 2008; 1236: 30–38.
13. Onda T, Honmou O, Harada K, Houkin K, Hamada H, Kocsis JD. Therapeutic benefits by human mesenchymal stem cells (hMSCs) and Ang-1 gene-modified hMSCs after cerebral ischemia. J. Cereb. Blood Flow Metab. 2008; 28: 329–340.



  

14. Toyama K, Honmou O, Harada K, Suzuki J, Houkin K, Hamada H, Kocsis JD. Therapeutic benefits of angiogenetic gene-modified human mesenchymal stem cells after cerebral ischemia. Exp. Neurol. 2009; 216: 47–55.
15. Nomura T, Honmou O, Harada K, Houkin K, Hamada H, Kocsis JD. I.V. infusion of brain-derived neurotrophic factor gene-modified human mesenchymal stem cells protects against injury in a cerebral ischemia model in adult rat. Neuroscience 2005; 136: 161–169.
16. Chen J, Li Y, Zhang R, Katakowski M, Gautam SC, Xu Y, Lu M, Zhang Z, Chopp M. Combination therapy of stroke in rats with a nitric oxide donor and human bone marrow stromal cells enhances angiogenesis and neurogenesis. Brain Res. 2004; 1005: 21–28.
17. Chen J, Zhang ZG, Li Y, Wang L, Xu YX, Gautam SC, Lu M, Zhu Z, Chopp M. Intravenous administration of human bone marrow stromal cells induces angiogenesis in the ischemic boundary zone after stroke in rats. Circ. Res. 2003; 92: 692–699.
18. Li Y, Chen J, Chen XG, Wang L, Gautam SC, Xu YX, Katakowski M, Zhang LJ, Lu M, Janakiraman N, Chopp M. Human marrow stromal cell therapy for stroke in rat: neurotrophins and functional recovery. Neurology 2002; 59: 514–523.
19. Zhang J, Li Y, Chen J, Yang M, Katakowski M, Lu M, Chopp M. Expression of insulin-like growth factor 1 and receptor in ischemic rats treated with human marrow stromal cells. Brain Res. 2004; 1030: 19–27.
20. Zhao LR, Duan WM, Reyes M, Keene CD, Verfaillie CM, Low WC. Human bone marrow stem cells exhibit neural phenotypes and ameliorate neurological deficits after grafting into the ischemic brain of rats. Exp. Neurol. 2002; 174: 11–20.
21. Dirnagl U, Iadecola C, Moskowitz MA. Pathobiology of ischaemic stroke: an integrated view. Trends Neurosci. 1999; 22: 391–397.
22. Plate KH. Mechanisms of angiogenesis in the brain. J. Neuropathol. Exp. Neurol. 1999; 58: 313–320.
23. Krupinski J, Kaluza J, Kumar P, Kumar S, Wang JM. Role of angiogenesis in patients with cerebral ischemic stroke. Stroke 1994; 25: 1794–1798.
24. Lin CY, Chang C, Cheung WM, Lin MH, Chen JJ, Hsu CY, Chen JH, Lin TN. Dynamic changes in vascular permeability, cerebral blood volume, vascular density, and size after transient focal cerebral ischemia in rats: evaluation with contrast-enhanced magnetic resonance imaging. J. Cereb. Blood Flow Metab. 2008; 28: 1491–1501.
25. Longa EZ, Weinstein PR, Carlson S, Cummins R. Reversible middle cerebral artery occlusion without craniectomy in rats. Stroke 1989; 20: 84–91.
26. Moriscot C, de Fraipont F, Richard MJ, Marchand M, Savatier P, Bosco D, Favrot M, Benhamou PY. Human bone marrow mesenchymal stem cells can express insulin and key transcription factors of the endocrine pancreas developmental pathway upon genetic and/or microenvironmental manipulation in vitro. Stem Cells 2005; 23: 594–603.
27. Detante O, Valable S, De Fraipont F, Grillon E, Barbier EL, Moisan A, Arnaud J, Moriscot C, Segebarth C, Hommel M, Rémy C, Richard M-J. MRI and fluorescence labeling of clinical grade mesenchymal stem cells without impacting their phenotype: study in a rat model of stroke. Stem Cells Translational Med. 2012. DOI: 10.5966/sctm.2011-0043.
28. Tropres I, Grimault S, Vaeth A, Grillon E, Julien C, Payen JF, Lamalle L, Decorps M. Vessel size imaging. Magn. Reson. Med. 2001; 45: 397–408.
29. Valable S, Lemasson B, Farion R, Beaumont M, Segebarth C, Remy C, Barbier EL. Assessment of blood volume, vessel size, and the expression of angiogenic factors in two rat glioma models: a longitudinal in vivo and ex vivo study. NMR Biomed. 2008; 21: 1043–1056.
30. Neumann-Haefelin T, Kastrup A, de Crespigny A, Yenari MA, Ringer T, Sun GH, Moseley ME. Serial MRI after transient focal cerebral ischemia in rats: dynamics of tissue injury, blood–brain barrier damage, and edema formation. Stroke 2000; 31: 1965–1972; discussion 1972–1973.
31. Beaumont M, Lemasson B, Farion R, Segebarth C, Remy C, Barbier EL. Characterization of tumor angiogenesis in rat brain using iron-based vessel size index MRI in combination with gadolinium-based dynamic contrast-enhanced MRI. J. Cereb. Blood Flow Metab. 2009; 29: 1714–1726.
32. Keunen O, Johansson M, Oudin A, Sanzey M, Rahim SA, Fack F, Thorsen F, Taxt T, Bartos M, Jirik R, Miletic H, Wang J, Stieber D, Stuhr L, Moen I, Rygh CB, Bjerkvig R, Niclou SP. Anti-VEGF treatment reduces blood supply and increases tumor cell invasion in glioblastoma. Proc. Natl. Acad. Sci. USA 2011; 108: 3749–3754.
33. Tropres I, Lamalle L, Peoc'h M, Farion R, Usson Y, Decorps M, Remy C. In vivo assessment of tumoral angiogenesis. Magn. Reson. Med. 2004; 51: 533–541.
34. Lemasson B, Christen T, Tizon X, Farion R, Fondraz N, Provent P, Segebarth C, Barbier EL, Genne P, Duchamp O, Remy C. Assessment of multiparametric MRI in a human glioma model to monitor cytotoxic and anti-angiogenic drug effects. NMR Biomed. 2010; 24: 473–482.
35. Pannetier N, Lemasson B, Christen T, Tachrount M, Tropres I, Farion R, Segebarth C, Remy C, Barbier EL. Vessel size index measurements in a rat model of glioma: comparison of the dynamic (Gd) and steady-state (iron-oxide) susceptibility contrast MRI approaches. NMR Biomed. 2012; 25: 218–226.
36. Lin TN, Sun SW, Cheung WM, Li F, Chang C. Dynamic changes in cerebral blood flow and angiogenesis after transient focal cerebral ischemia in rats. Evaluation with serial magnetic resonance imaging. Stroke 2002; 33: 2985–2891.
37. Komatsu K, Honmou O, Suzuki J, Houkin K, Hamada H, Kocsis JD. Therapeutic time window of mesenchymal stem cells derived from bone marrow after cerebral ischemia. Brain Res. 2010; 1334: 84–92.
38. Kode JA, Mukherjee S, Joglekar MV, Hardikar AA. Mesenchymal stem cells: immunobiology and role in immunomodulation and tissue regeneration. Cytotherapy 2009; 11: 377–391.
39. Sanz L, Santos-Valle P, Alonso-Camino V, Salas C, Serrano A, Vicario JL, Cuesta AM, Compte M, Sanchez-Martin D, Alvarez-Vallina L. Long-term in vivo imaging of human angiogenesis: critical role of bone marrow-derived mesenchymal stem cells for the generation of durable blood vessels. Microvasc. Res. 2008; 75: 308–314.
40. Caplan AI, Dennis JE. Mesenchymal stem cells as trophic mediators. J. Cell. Biochem. 2006; 98: 1076–1084.
41. Au P, Tam J, Fukumura D, Jain RK. Bone marrow-derived mesenchymal stem cells facilitate engineering of long-lasting functional vasculature. Blood 2008; 111: 4551–4558.
42. Kojima T, Hirota Y, Ema M, Takahashi S, Miyoshi I, Okano H, Sawamoto K. Subventricular zone-derived neural progenitor cells migrate along a blood vessel scaffold toward the post-stroke striatum. Stem Cells 2010; 28: 545–554.
43. Ohab JJ, Fleming S, Blesch A, Carmichael ST. A neurovascular niche for neurogenesis after stroke. J. Neurosci. 2006; 26: 13 007–13 016.
44. Aggarwal S, Pittenger MF. Human mesenchymal stem cells modulate allogeneic immune cell responses. Blood 2005; 105: 1815–1822.
45. Witte OW, Stoll G. Delayed and remote effects of focal cortical infarctions: secondary damage and reactive plasticity. Adv. Neurol. 1997; 73: 207–227.
46. Manoonkitiwongsa PS, Jackson-Friedman C, McMillan PJ, Schultz RL, Lyden PD. Angiogenesis after stroke is correlated with increased numbers of macrophages: the clean-up hypothesis. J. Cereb. Blood Flow Metab. 2001; 21: 1223–1231.
47. Yu SW, Friedman B, Cheng Q, Lyden PD. Stroke-evoked angiogenesis results in a transient population of microvessels. J. Cereb. Blood Flow Metab. 2007; 27: 755–763.